15(S)-hydroxyeicosatetraenoic acid–induced angiogenesis requires Src-mediated Egr-1–dependent rapid induction of FGF-2 expression

Venkatesh Kundumani-Sridharan,[1] Jixiao Niu,[1] Dong Wang,[1] Dong Van Quyen,[1] Qiuhua Zhang,[1] Nikhlesh K. Singh,[1] Jaganathan Subramani,[1] Saradasri Karri,[1] and Gadiparthi N. Rao[1]

[1]Department of Physiology, University of Tennessee Health Science Center, Memphis

To understand the mechanisms underlying 15(S)-hydroxyeicosatetraenoic acid [15(S)-HETE]–induced angiogenesis, we studied the role of Egr-1. 15(S)-HETE induced Egr-1 expression in a time-dependent manner in human dermal microvascular endothelial cells (HDMVECs). Blockade of Egr-1 via forced expression of its dominant-negative mutant attenuated 15(S)-HETE–induced HDMVEC migration and tube formation as well as Matrigel plug angiogenesis. 15(S)-HETE–induced Egr-1 expression requires Src activation. In addition, adenovirus-mediated expression of dominant-negative mutant of Src blocked 15(S)-HETE's effects on migration and tube formation of HDMVECs and Matrigel plug angiogenesis. 15(S)-HETE induced fibroblast growth factor-2 (FGF-2) expression rapidly via Src-mediated production of Egr-1. Cloning and mutational analysis of FGF-2 promoter revealed that Egr-1 binding site proximal to transcription start site is required for 15(S)-HETE–induced FGF-2 expression. Neutralizing antibody-mediated suppression of FGF-2 function also attenuated the effects of 15(S)-HETE on HDMVEC migration and tube formation as well as Matrigel plug angiogenesis. Furthermore, in contrast to wild-type mice, 12/15-LOX$^{-/-}$ mice exhibited decreased Matrigel plug angiogenesis in response to AA, which was rescued by 15(S)-HETE. On the basis of these observations, we conclude that 15(S)-HETE–induced angiogenesis requires Src-mediated Egr-1–dependent rapid induction of FGF-2. These findings may suggest that 15(S)-HETE could be a potential endogenous regulator of pathologic angiogenesis associated with atherosclerosis and restenosis. (Blood. 2010;115:2105-2116)

Introduction

Between the two 15-lipoxygenases (15-LOXs), 15-LOX1 converts arachidonic acid (AA) majorly to 15(S)-hydroxyeicosatetraenoic acid [15(S)-HETE] and minorly to 12(S)-HETE.[1,2] 15-LOX2, however, metabolizes AA exclusively to 15(S)-HETE.[2,3] Both 15-LOX1 and 15-LOX2 are present in humans.[4] Opposite actions have been observed for 15-LOX1 and 15-LOX2 in influencing prostate cancer, the former being procarcinogenic.[5-8] However, in these responses 12(S)-HETE mimicked 15-LOX1, whereas 15(S)-HETE exhibited effects similar to 15-LOX2.[9-11] Specifically, although 15-LOX1-12(S)-HETE appears to exert procarcinogenic effects, 15-LOX2-15(S)-HETE exhibited proapoptotic actions in prostate carcinomas. However, in the case of colorectal carcinomas, 15-LOX1 induced apoptosis.[12,13] It was demonstrated that 15-LOX mediates oxidation of low-density lipoprotein, a factor that appears to be crucial in the pathogenesis of atherosclerosis.[14,15] In addition, atherosclerotic arteries upon incubation ex vivo converted AA mainly to 15-HETE.[16] Knockout mice for 12/15-LOX, a murine ortholog of 15-LOX1, exhibited decreased atherosclerotic lesions in response to a high-fat diet and reduced neointima formation in response to injury.[17,18] Conversely, overexpression of 15-LOX1 in vascular endothelium enhanced atherosclerosis in low-density lipoprotein receptor-deficient mice.[19]

These results suggest a role for 15-LOX1-15(S)-HETE/12/15-LOX-12(S)-HETE axis in vascular diseases. In regard to other diseases, particularly, retinopathy, 15(S)-HETE levels have been found to be elevated in epiretinal membranes of proliferative vitreoretinal and proliferative diabetic retinopathy patients.[20] Furthermore, hypoxia increased the expression of 15-LOX1 and production of 15(S)-HETE in pulmonary arteries, causing vasoconstriction.[21] Hypoxia also increased the production of 15(S)-HETE in human retinal microvascular endothelial cells, causing angiogenesis.[22-24] In addition, we showed that 15(S)-HETE–induced angiogenesis requires phosphoinositide 3-kinase-Akt–dependent fibroblast growth factor-2 (FGF-2) expression and signal transducer and activator of transcription-3–mediated vascular endothelial growth factor expression.[25,26]

Egr-1, a zinc finger transcriptional factor, has been shown to play an important role in the regulation of cell migration and proliferation.[27,28] In addition, the involvement of Egr-1 in the pathogenesis of various diseases, including vascular diseases, has been demonstrated.[29-31] In many reports[32,33] authors have demonstrated that Egr-1 mediates the expression of angiogenic factors such as FGF-2 and antiangiogenic factors such as thrombospondin I in response to several cues. Because angiogenesis appears to be involved in atherosclerosis and restenosis[34,35] and because both 15(S)-HETE and Egr-1 possess the capacity to modulate angiogenesis[23-26,29] and both molecules are produced in these vascular lesions,[16,30] we asked the question whether Egr-1 plays a role in 15(S)-HETE–induced angiogenesis. We found that 15(S)-HETE induces the expression of Egr-1 in human dermal microvascular endothelial cells (HDMVECs) and that this effect is dependent on activation of Src. In addition, 15(S)-HETE–induced angiogenesis

requires Egr-1–mediated rapid expression of FGF-2. Furthermore, AA, although inducing robust angiogenesis in wild-type (WT) mice, failed to influence a similar effect in 12/15-LOX$^{-/-}$ mice, suggesting the importance of AA metabolism via the lipoxygenase pathway in the regulation of angiogenesis.

Methods

Reagents

15(S)-HETE and 15(S)-HETE enzyme immunoassay (EIA) kit were bought from Cayman Chemicals. Growth factor-reduced Matrigel and anti-CD31 antibodies were obtained from BD Biosciences. Phosphospecific anti-Src antibodies were from Cell Signaling Technology. Anti-Src antibodies were obtained from Upstate Biotechnology Inc. Anti–Egr-1 antibodies (SC-189), anti–FGF-2 antibodies (SC-79), anti–β-tubulin antibodies (SC-9104), and normal mouse serum (SC-2025) were purchased from Santa Cruz Biotechnology Inc. Neutralizing anti–FGF-2 antibodies were bought from Millipore. A human FGF-2 enzyme-linked immunosorbent assay (ELISA) kit was obtained from R&D Systems. Anti–von Willebrand Factor (vWF) antibodies were supplied by Abcam. Hoechst 33342 (H3570) and Prolong Gold antifade mounting medium (P36930) were bought from Invitrogen. T4 polynucleotide kinase was procured from New England Biolabs. [γ^{32}P]-ATP (3000 Ci/mmol) was bought from GE Healthcare Biosciences. All of the primers were made by IDT.

Adenoviral vectors

To construct adenoviral vector for dnEgr-1, its cDNA was released from pCB6-Egr-1 plasmid by digestion with *Hin*dIII and *Sma*I and cloned into the same sites of pBluescript vector. DnEgr-1 cDNA was retrieved from pBluescript vector by digestion with *Kpn*I and *Not*I and subcloned into the same sites of entry vector pENTR3C. The pAd-dnEgr-1 was generated by specific recombination of pENTR3C-dnEgr-1 with pAdCMV5DEST (Invitrogen). The plasmid pAd-dnEgr-1 was linearized by digestion with *Pac*I and transfected into HEK293A cells to amplify Ad-dnEgr-1 virus. The dominant-negative Egr-1 contains transcriptional repressor domain of Wilms tumor protein (aa 1-307) at the N-terminus of Egr-1 DNA binding domain (aa 327-427).[36] Construction of Ad-GFP and Ad-dnSrc was described previously.[37] Adenovirus was purified with cesium chloride centrifugation, and the titer was determined by plaque assay, as described previously.[37]

Cell culture

HDMVECs were bought from Cascade Biologics and grown in medium 131 containing microvascular growth supplements, 10 μg/mL gentamicin, and 0.25 μg/mL amphotericin B. Cultures were maintained at 37°C in a humidified 95% air and 5% CO_2 atmosphere. HDMVECs were growth-arrested by incubating in medium 131 for 24 hours and used to perform the experiments unless otherwise indicated.

Cell migration

Cell migration was performed by the use of the modified Boyden Chamber method as described by us previously.[38] The cell culture inserts containing membranes with 10 mm in diameter and 8.0-μm pore size (Nalgene Nunc International) were placed in a 24-well tissue culture plate (Costar; Corning Inc). The lower surface of the porous membrane was coated with 70% Matrigel at 4°C overnight and then blocked with 0.1% heat-inactivated bovine serum albumin at 37°C for 1 hour. HDMVECs were quiesced for 24 hours in medium 131, trypsinized, and neutralized with trypsin-neutralizing solution. Cells were seeded into the upper chamber at 10^5 cells/well. Vehicle or 15(S)-HETE was added to the lower chamber. Both the upper and lower chambers contained medium 131. When the effect of dominant-negative Src and Egr-1 mutants was tested on 15(S)-HETE–induced HDMVEC migration, cells were infected first with Ad-GFP, Ad-dnSrc, or Ad-dnEgr-1 at 40 multiplicity of infection (moi) and quiesced before they were subjected to migration assay. In the case of testing the effect of neutralizing anti–FGF-2 antibodies on 15(S)-HETE–induced HDMVEC migration, cells were incubated with antibodies (3 μg/mL) for 30 minutes at 37°C followed by washing with medium 131. Cells were then seeded into each well, and wherever appropriate, the antibodies were added to both the upper and lower chambers before the addition of 15(S)-HETE. After 6 hours of incubation at 37°C, nonmigrated cells were removed from the upper side of the membrane with cotton swabs and the cells on the lower surface of the membrane were fixed in methanol for 15 minutes. The membrane was then stained with DAPI in VECTASHIELD mounting medium (Vector Laboratories Inc) and observed under Nikon diaphot fluorescence microscope with photometrics CH250 CCD camera (Nikon). Cells were counted in 5 randomly selected squares per well and presented as number of migrated cells per field.

Tube formation

Tube formation assay was performed as described by us previously.[38] Twenty-four-well culture plates (Costar; Corning Inc) were coated with growth factor-reduced Matrigel (BD Biosciences) in a total volume of 280 μL/well and allowed to solidify for 30 minutes at 37°C. HDMVECs were trypsinized, neutralized with TNS, and resuspended at 5×10^5 cells/mL, and 200 μL of this cell suspension was added into each well. Vehicle or 15(S)-HETE, at the indicated concentration, was added to the appropriate well, and the cells were incubated at 37°C for 6 hours. When the effect of dominant-negative Src and Egr-1 mutants was tested on 15(S)-HETE–induced HDMVEC tube formation, cells were infected first with Ad-GFP, Ad-dnSrc, or Ad-dnEgr-1 at 40 moi and quiesced before they were subjected to tube formation. In the case of testing the effect of neutralizing anti–FGF-2 antibodies on 15(S)-HETE–induced HDMVEC tube formation, cells were incubated with antibodies (3 μg/mL) for 30 minutes at 37°C followed by washing with medium 131. Cells were then seeded into each well, and wherever appropriate, the antibodies were added to the well before the addition of 15(S)-HETE. Tube formation was observed under an inverted microscope (Eclipse TS100; Nikon). Images were captured with a CCD color camera (KP-D20AU; Hitachi) attached to the microscope and tube length was measured with National Institutes of Health (NIH) Image J.

Western blotting

After appropriate treatments and rinsing with cold phosphate-buffered saline (PBS), HDMVECs were lysed in 500 μL of lysis buffer (PBS, 1% Nonidet P-40, 0.5% sodium deoxycholate, 0.1% sodium dodecyl sulfate [SDS], 100 μg/mL phenylmethylsulphonyl fluoride, 100 μg/mL aprotinin, 1 μg/mL leupeptin, and 1mM sodium orthovanadate) and scraped into 1.5-mL Eppendorf tubes. After standing on ice for 20 minutes, the cell lysates were cleared by centrifugation at 13 000g for 20 minutes at 4°C. Cell lysates containing equal amount of protein were resolved by electrophoresis on 0.1% SDS and 10% polyacrylamide gels. The proteins were transferred electrophoretically to a nitrocellulose membrane (Hybond; Amersham Pharmacia Biotech). After blocking in 10mM Tris-HCl buffer (pH 8.0) containing 150mM sodium chloride, 0.1% Tween 20, and 5% (wt/vol) nonfat dry milk, the membrane was treated with appropriate primary antibodies followed by incubation with horseradish peroxidase-conjugated secondary antibodies. The antigen-antibody complexes were detected with the use of a chemiluminescence reagent kit (Amersham Pharmacia Biotech). The band intensities were quantified with NIH Image J1.31v program.

Quantitative RT-PCR

After appropriate treatments, total cellular RNA was isolated from HDMVECs by the use of Trizol reagent as per the manufacture's guidelines (Invitrogen). Reverse transcription (RT) was carried out with Superscript III First-Strand Synthesis System for RT-polymerase chain reaction (PCR) on
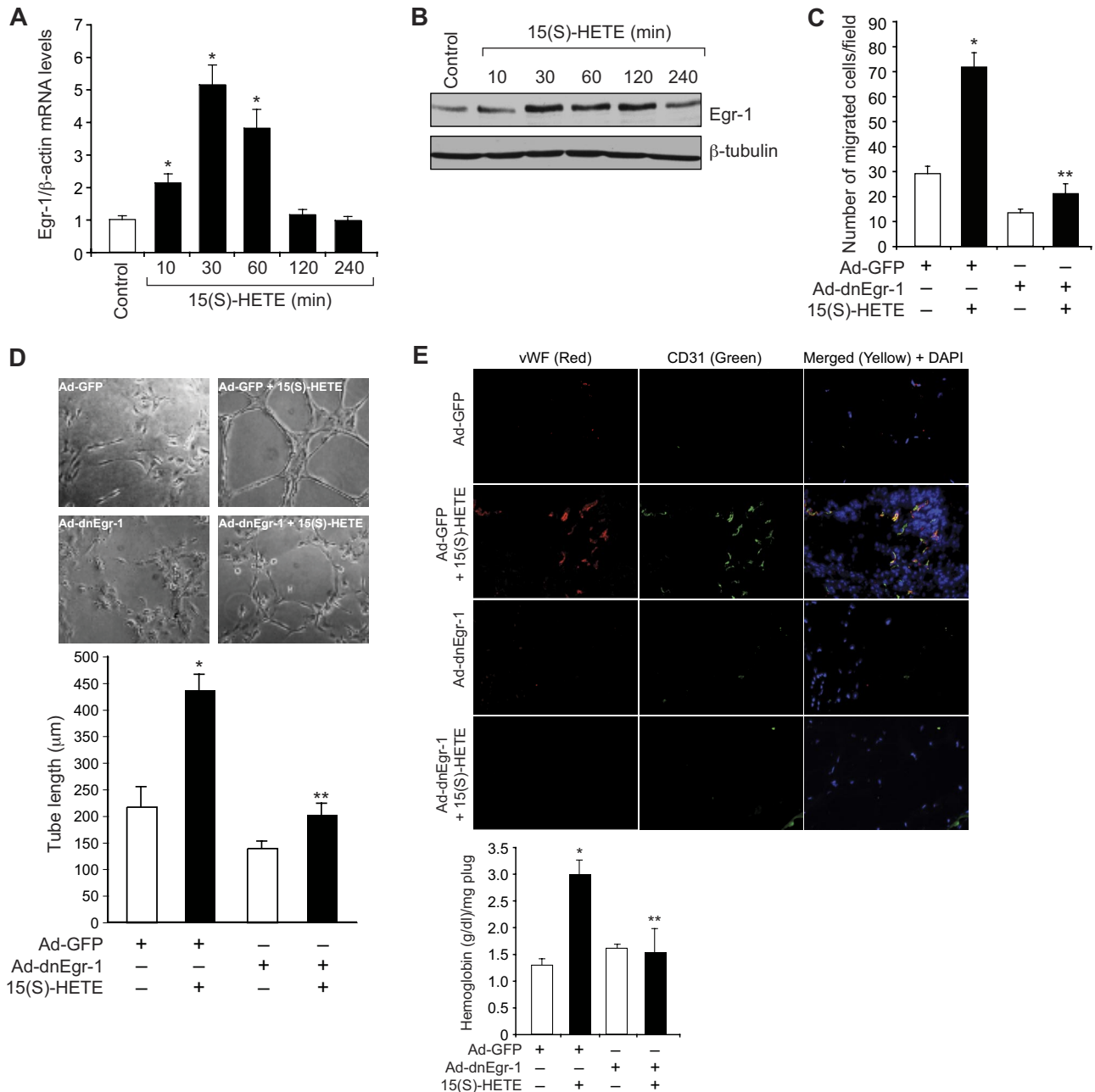
Figure 1. Egr-1 mediates 15(S)-HETE–induced HDMVEC migration and tube-like structure formation in vitro and Matrigel plug angiogenesis in vivo. (A-B) Quiescent human dermal microvascular endothelial cells (HDMVECs) were treated with and without 15(S)-hydroxyeicosatetraenoic acid (15(S)-HETE; 0.1μM) for the indicated time periods, and either RNA was isolated or cell extracts were prepared. (A) RNA was analyzed by QRT-PCR for Egr-1 and β-actin mRNA levels. (B) Cell extracts were analyzed by Western blotting for Egr-1 levels by the use of its specific antibodies. The blot was reprobed with anti–β-tubulin antibodies for normalization. (C-D) HDMVECs were transduced with Ad-GFP or Ad-dnEgr-1 at a moi of 40, quiesced, and subjected to 15(S)-HETE–induced migration (C) or tube-like structure formation (D). (E) C57BL/6 mice were injected subcutaneously with 0.5 mL of Matrigel premixed with vehicle or 5μM 15(S)-HETE along with and without Ad-GFP or Ad-dnEgr-1 (5 × 10⁹ pfu/mL). One week later, the animals were sacrificed, and the Matrigel plugs were harvested from underneath the skin and either processed for von Willebrand Factor (vWF) and CD31 expression by double immunofluorescence staining with their specific antibodies or analyzed for hemoglobin content with Drabkin reagent. The bar graphs in panels A, C, D, and E represent the quantitative analysis of 3 independent experiments or 6 plugs from 6 animals. The values are presented as the mean ± SD. *$P <$ .01 vs control or Ad-GFP; **$P <$ .01 vs Ad-GFP + 15(S)-HETE.

the basis of the supplier's protocol (Invitrogen). The cDNA was then used as template for PCR with Taqman Gene Expression Assay kit for human Egr-1, human FGF-2, and human β-actin. The amplification was carried out on Applied Biosystems 7300 Real-Time PCR System (Applied Biosystems), with the use of the following amplification conditions for the aforementioned genes as follows: 95°C for 10 minutes followed by 40 cycles at 95°C for 15 seconds with extension at 60°C for 1 minute. The amplification was examined with the use of the 7300 Real-Time PCR System-SDS, Version 1.4, program.

Cloning of human FGF-2 promoter-luciferase reporter constructs

The human FGF-2 promoter was cloned from human genomic DNA by nested PCR method. The promoter was initially amplified by the outer sense primer, 5′-TAG GGC AAA TGC CAG GTC CGA GTT AAG-3′ (hFGF2p-S), and the antisense primer, 5′-AAG CTT GGC GTC ACA TCT TCT ACA TCT CCA CCC-3′ (hFGF2p-R). The resulting PCR product was then used as a template to amplify the internal region encompassing nucleotides from
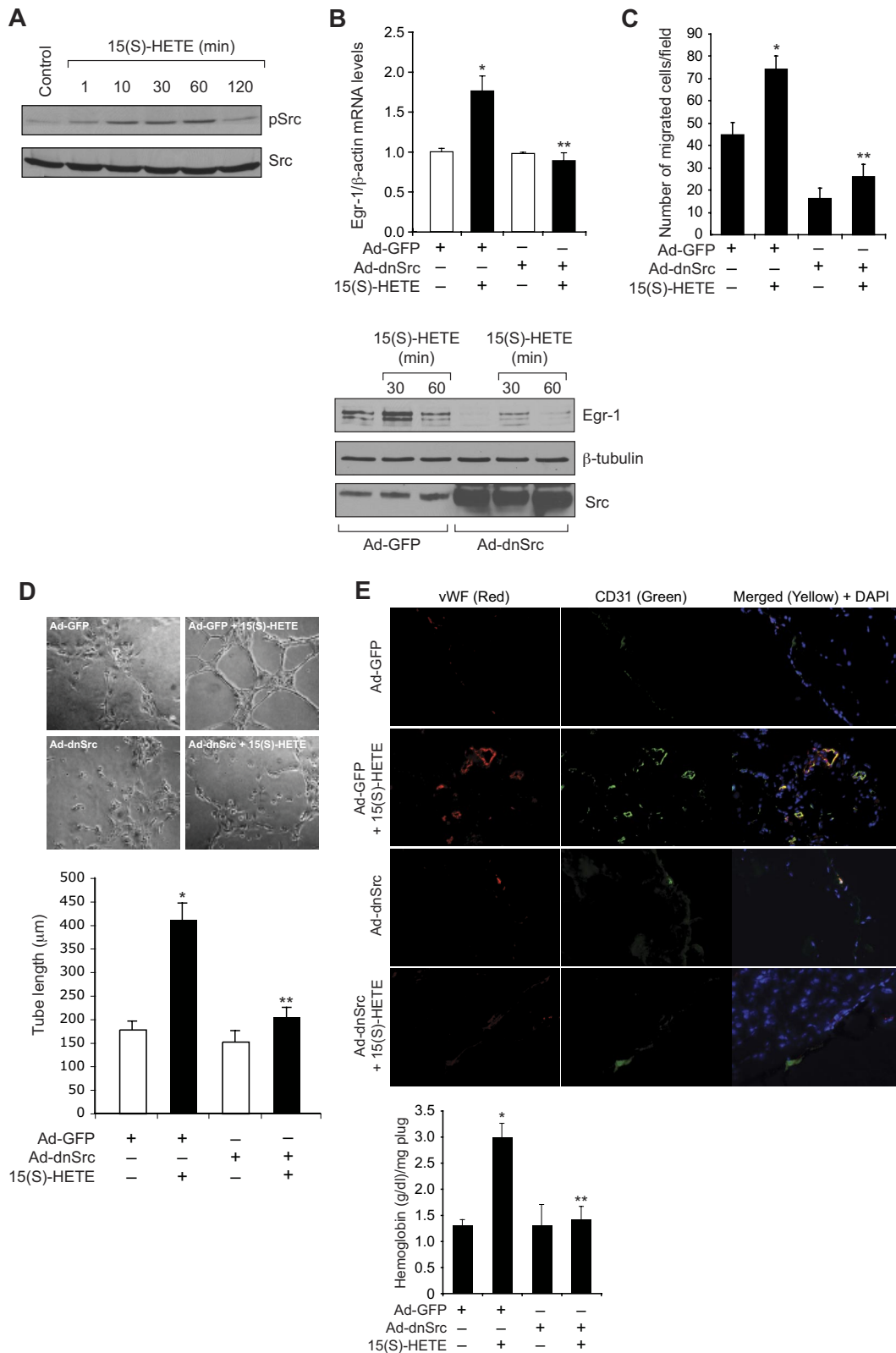
Figure 2. Src mediates 15(S)-HETE–induced Egr-1 expression in HDMVECs, leading to their migration and tube-like structure formation. (A) Quiescent HDMVECs were treated with and without 15(S)-HETE (0.1μM) for the indicated time periods, and cell extracts were prepared and analyzed by Western blotting for pSrc with the use of its phosphospecific antibodies. The blot was reprobed with anti-Src antibodies for normalization. (B) HDMVECs were transduced with Ad-GFP or Ad-dnSrc at a moi of 40, quiesced, and treated with and without 15(S)-HETE (0.1μM) for either 30 minutes for RNA isolation or 30 minutes and 60 minutes for cell extract preparation. RNA was analyzed for Egr-1 and β- actin mRNA levels by QRT-PCR, and cell extracts were analyzed by Western blotting for Egr-1 with the use of its specific antibodies. The blot was reprobed sequentially with anti–β-tubulin antibodies and anti-Src antibodies for normalization and to show the overexpression of dnSrc, respectively. (C-D) HDMVECs that were transduced with Ad-GFP or Ad-dnSrc at a moi of 40 and quiesced were subjected to 15(S)-HETE (0.1μM)–induced migration (C) or tube-like structure formation (D). (E) C57BL/6 mice were injected subcutaneously with 0.5 mL of Matrigel premixed with vehicle or 5μM 15(S)-HETE in combination with and without Ad-GFP or Ad-dnSrc (5×10^9 pfu/mL). One week later, the animals were sacrificed, and the Matrigel plugs were harvested from underneath the skin and either processed for vWF and CD31 expression by double immunofluorescence staining with their specific antibodies or analyzed for hemoglobin content using Drabkin reagent. The bar graphs in panels B, C, D, and E represent the quantitative analysis of 3 independent experiments or 6 plugs from 6 animals. The values are presented as the mean ± SD. *$P < .01$ vs Ad-GFP; **$P < .01$ vs Ad-GFP + 15(S)-HETE.
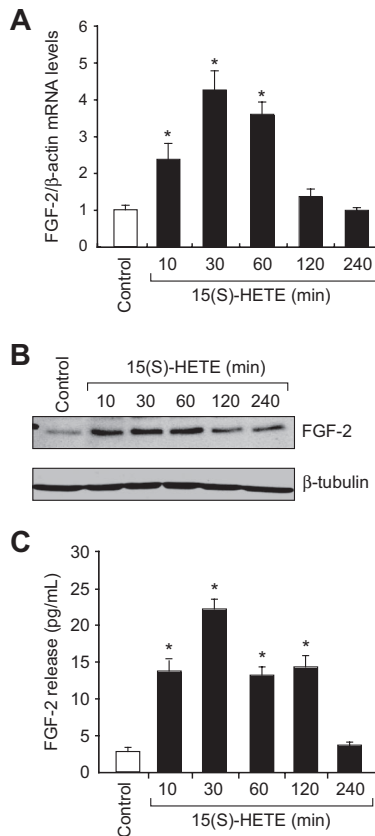
Figure 3. 15(S)-HETE induces FGF-2 expression rapidly in HDMVECs. (A-B) Quiescent HDMVECs were treated with and without 15(S)-HETE (0.1μM) for various time periods, and either RNA was isolated or cell extracts were prepared. RNA was analyzed by QRT-PCR for FGF-2 and β-actin mRNA levels, and cell extracts were analyzed by Western blotting for FGF-2 levels with the use of its specific antibodies. The blot was reprobed with anti–β-tubulin antibodies for normalization. (C) All the conditions were the same as in panel B except that medium was collected and analyzed for FGF-2 release by ELISA. The bar graphs in panels A and C represent the quantitative analysis of 3 independent experiments. The values are presented as the means ± SD. *$P < .01$ vs control.

−494 to +125 relative to the transcription start site with an inner sense primer, 5′-CCC CTC GAG CTC CCC TTC TCT GGC CTC T-3′ (hFGF2p-F) incorporating a *Xho*I restriction enzyme site at the 5′-end and the outer reverse primer, hFGF2p-R, incorporating a *Hin*dIII restriction enzyme site at the 5′-end.

The PCR products were subcloned into the pGEM-T vector, sequenced, and then released from the vector by digestion with *Xho*I and *Hin*dIII. The released fragments were cloned into *Xho*I and *Hin*dIII sites of the pGL3 basic vector (Promega) to yield hFGF2p-wt-Luc. Site-directed mutagenesis of the Egr-1 binding sites was done by a PCR-based overlap extension method with the hFGF2p-wt-Luc as a template. The hFGF2p-F and hFGF2p-R were used as external primers in combination with following primers incorporating mutations, forward, 5′-TGG TGC GGG GGT TGG **GTT AAG** GTG ACT TTT GGG GGA-3′ (Egr1-M2-F) and reverse, 5′-TCC CCC AAA AGT CAC **CTT AAC** CCA ACC CCC GCA CCA-3′ (Egr1-M2-R); forward, 5′-CCC TCG CCT CTC CCC **CTT AAC** CGA CTG AGG CCG GGC T-3′ (Egr1-M1-F) and reverse, 5′-AGC CCG GCC TCA GTC GG**T TAA** GGG GGA GAG GCG AGG G-3′ (Egr1-M1-R) for generation of mutated reporter constructs targeting Egr-1 sites at −165 and −65 nt, respectively. The bold letters indicate the mutations. The constructs were confirmed by restriction enzyme analysis and DNA sequencing.

Luciferase assay

HDMVECs were transfected with FGF-2 promoter-luciferase constructs or pGL3 basic vector with Lipofectamine 2000 reagent. After growth synchro-nization in growth factor-free medium for 12 hours, cells were treated with and without 15(S)-HETE (0.1μM) for 30 minutes. Cells were then washed once with ice-cold PBS and lysed with 200 μL of lysis buffer. The cell extracts were collected into microcentrifuge tubes and centrifuged for 2 minutes at 12 000g at 4°C. The supernatants were collected and assayed for luciferase activity with the Luciferase Assay System (Promega) and a single-tube luminometer (TD20/20 Turner Designs), and the values are expressed as relative luciferase units.

Electrophoretic mobility shift assay

After appropriate treatments, nuclear extracts were prepared from HDM-VECs as described previously.[26] The protein content of the nuclear extracts was determined with the use of a Micro BCA Protein Assay Reagent Kit (Pierce). Protein-DNA complexes were formed by incubating 10 μg of nuclear protein in a total volume of 25 μL consisting of 1mM HEPES (N-2-hydroxyethylpiperazine-N′-2-ethanesulfonic acid), pH 7.9; 3mM Tris-HCl, pH 7.9; 60mM KCl; 1mM EDTA (ethylenediaminetetraacetic acid); 1mM phenylmethylsulphonyl fluoride; 1mM dithiothreitol; 2.5 μg/mL bovine serum albumin; 1 μg/mL poly (dI-dC), 15% glycerol, and 100,000 cpm of [32P]-labeled oligonucleotide probe for 30 minutes on ice. The protein-DNA complexes were resolved by electrophoresis on a 4% polyacrylamide gel with the use of 1X Tris-glycine-EDTA buffer (25mM Tris-HCl, pH 8.5; 200mM glycine; 0.1mM EDTA). Double-stranded oligo-nucleotides (5′-CGCCTCTCCCCCGCCCCCGACTGAG-3′, 3′-GCG-GAGAGGGGGCGGGGGCTGACTC-5′) encompassing a Egr-1 binding sequence from −57 to −65 region of human FGF-2 promoter (accession no. S81809) were used as [32P]-labeled probe to measure Egr-1 DNA binding activity. Double-stranded oligonucleotides were labeled with [γ32P]-ATP with the T4 polynucleotide kinase kit following the sup-plier's protocol.

ChIP

Chromatin immunoprecipitation (ChIP) assay was performed on HDM-VECs by use of the ChIP assay kit following supplier's protocol (Upstate Biotechnology Inc). Egr-1-DNA complexes were immunoprecipitated with an anti–Egr-1 antibody. Preimmune rabbit serum was used as a negative control. The immunoprecipitated DNA was uncross-linked, subjected to Proteinase K digestion, and purified with QIAquick columns (QIAGEN). The purified DNA was used as a template for PCR amplification by the use of primers (forward, 5′-AAGCCTGCTCTGACACAGAC-3′; reverse, 5′-GTTCGGCCACAACACGCAA-3′) flanking the putative Egr-1–binding site located at −57 to −65 nt in human FGF-2 promoter region (accession no. S81809). The PCR products were resolved on 1.2% agarose gel, stained with ethidium bromide, and the band intensities were quantified by the use of NIH Image J.

Matrigel plug angiogenesis

All the experiments that used animals were performed in accordance with the relevant guidelines and regulations approved by the Institutional Animal Care and Use Committee of the University of Tennessee Health Science Center. Matrigel plug assay was performed essentially as described by us previously.[37] The C57BL/6 and 12/15-LOX$^{-/-}$ mice were obtained from The Jackson Laboratory. C57BL/6 mice or 12/15-LOX$^{-/-}$ mice (8 weeks old) were lightly anesthetized with sodium pentobarbital (50 mg/kg intra-peritoneally) and were injected subcutaneously with 0.5 mL of Matrigel that was premixed with vehicle or 5μM of either AA or 15(S)-HETE along the abdominal midline. The injections were made rapidly with a B-D 30G1/2 needle to ensure the entire content was delivered as a single plug. Wherever the effect of Ad-GFP (5×10^9 pfu/mL), Ad-dnSrc (5×10^9 pfu/mL), Ad-dnEgr-1 (5×10^9 pfu/mL), preimmune serum (20 μg/mL), or neutralizing anti–FGF-2 antibodies (20 μg/mL) was tested on 15(S)-HETE–induced angiogenesis, they were added to the Matrigel before injecting into mice.

The mice were allowed to recover, and 7 days later, unless otherwise stated, the animals were sacrificed by inhalation of CO_2 and the Matrigel
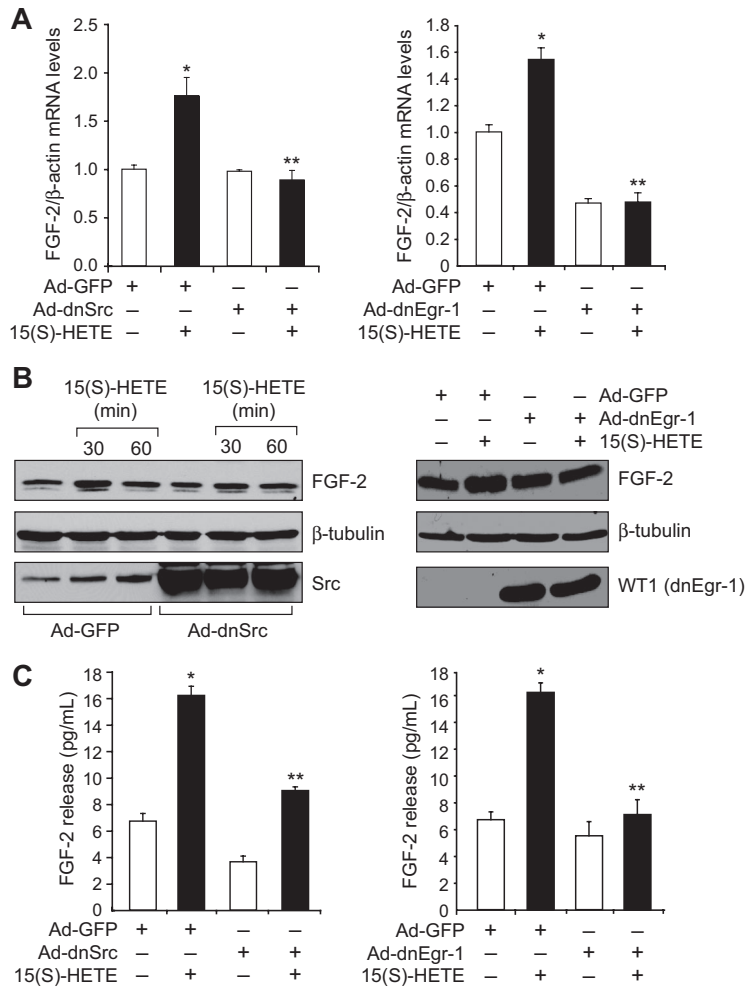
A

B

C

Figure 4. 15(S)-HETE–induced FGF-2 expression is mediated by Src-Egr-1 signaling in HDMVECs. (A-B) HDMVECs were transduced with Ad-GFP, Ad-dnSrc, or Ad-dnEgr-1 with a moi of 40, quiesced, and treated with and without 15(S)-HETE (0.1μM) for either 30 minutes for RNA isolation or 30 minutes and/or 60 minutes for cell extract preparation. RNA was analyzed by QRT-PCR for FGF-2 and β-actin mRNA levels, and cell extracts were analyzed by Western blotting for FGF-2 levels with its specific antibodies. The blots were reprobed with anti–β-tubulin antibodies and/or anti-Src antibodies or anti-WT1 antibodies for normalization and to show overexpression of dnSrc or dnEgr-1, respectively. (C) All the conditions were the same as in panel A except that medium was collected and tested for FGF-2 release by ELISA. The bar graphs in panels A and C represent the quantitative analysis of 3 independent experiments. The values are presented as the means ± SD. *$P < .01$ vs Ad-GFP; **$P < .01$ vs Ad-GFP + 15(S)-HETE.

plugs were harvested from underneath the skin. The plugs were homogenized in 1 mL of deionized H_2O on ice and cleared by centrifugation at 9000g for 6 minutes at 4°C. The supernatant was collected and used in duplicate to measure hemoglobin content with Drabkin reagent along with hemoglobin standard essentially according to the manufacturer's protocol (Sigma-Aldrich). The absorbance was read at 540 nm in an ELISA plate reader (Spectra Max 190; Molecular Devices). These experiments were repeated at least 3 times with 6 mice for each group, and the values are expressed as grams of hemoglobin per deciliter per milligram of plug.

Double immunofluorescence staining

After retrieving the Matrigel plugs from mice, they were snap-frozen in OCT compound. Cryosections (5 μm) were made with the use of Leica Kryostat (CM3050S; Leica). After blocking in goat serum, the cryosections were incubated with rabbit anti–mouse vWF antibodies and rat anti–mouse CD31 antibodies for 1 hour. After washing in PBS, all slides were incubated with tetramethylrhodamine isothiocyanate-conjugated goat anti–rabbit and fluorescein-conjugated goat anti–rat secondary antibodies. In the case of negative control, incubation with primary antibodies was omitted. Fluorescence images of the Matrigel sections were captured by the use of an inverted Zeiss fluorescence microscope, (AxioVision AX10) via a 10×/0.6 numeric aperture objective and AxioCam MRm camera without any enhancements.

ELISA

FGF-2 released into the culture medium was measured with the use of an ELISA kit following the manufacturer's instructions (R&D Systems).

EIA

At 7 days after Matrigel injection, the plugs were retrieved from mice, minced, and incubated with AA (10μM) along with ionomycin (10μM) for 3 hours. The eicosanoids were extracted with 10% (vol/vol) methanol. After adjusting the pH to 2.5 with 10% (vol/vol) glacial acetic acid, the mixture was passed through Pre-Sep C18 column. The eicosanoids were eluted with 100% methanol followed by evaporation to dryness and then reconstituted in 50 μL of EIA buffer (Cayman Chemicals). 15(S)-HETE was assayed with the use of 15(S)-HETE EIA kit following the manufacturer's (Cayman Chemicals) instructions.

Statistics

All the experiments were repeated 3 times, and data are presented as mean plus or minus SD. The treatment effects were analyzed by the Student t test, and P values less than .05 were considered to be statistically significant. In the case of ChIP assay, double immunofluorescence staining, electrophoretic mobility shift assay (EMSA), and Western blotting analysis, 1 representative set of data are shown.

Results

Previously we showed that 15(S)-HETE, a major AA metabolite of 15-LOX1/2, plays a role in the induction of angiogenesis.[24-26,38] To understand the mechanisms underlying 15(S)-HETE–induced angiogenesis, we have studied the role of Egr-1, a zinc finger

A

```
-493  CTCCCCTTCT CTGGCCTCTT TCTCTCCTTT TGTTGGTAGA CGACTTCAGC CTCTGTCCTT TAATTTTAAA

-423  GTTTATGCCC CACTTGTACC CCTCGTCTTT TGGTGATTTA GAGATTTTCA AAGCCTGCTC TGACACAGAC

-353  TCTTCCTTGG ATTGCAACTT CTCTACTTTG GGGTGGAAAC GGCTTCTCCG TTTTGAAACG CTAGCGGGGA

-283  AAAAATGGGG GAGAAAGTTG AGTTTAAACT TTTAAAAGTT GAGTCACGGC TGGTTGCGCA GCAAAAGCCC
                                                                         Egr-1
-213  CGCAGTGTGG AGAAAGCCTA AACGTGGTTT GGGTGGTGCG GGGGTTGG**GC GGGGGTG**ACT TTTGGGGGAT

-143  AAGGGGCGGT GGAGCCCAGG GAATGCCAAA GCCCTGCCGC GGCCTCCGAC GCGCGCCCCC CGCCCCTCGC
                        Egr-1
-73   CTCTCCCC**CG CCCCCGA**CTG AGGCCGGGCT CCCCGCCGGA CTGATGTCGC GCGCTTGCGT GTTGTGGCCG

-3    AACCGCCGAA CTCAGAGGCC GGCCCCAGAA AACCCGAGCG AGTAGGGGGC GGCGCGCAGG AGGGAGGAGA
        →
        +1
+68   ACTGGGGGCG CGGGAGGCTG GTGGGTGTGG GGGGTGGAGA TGTAGAAGAT GTGACGCC
```
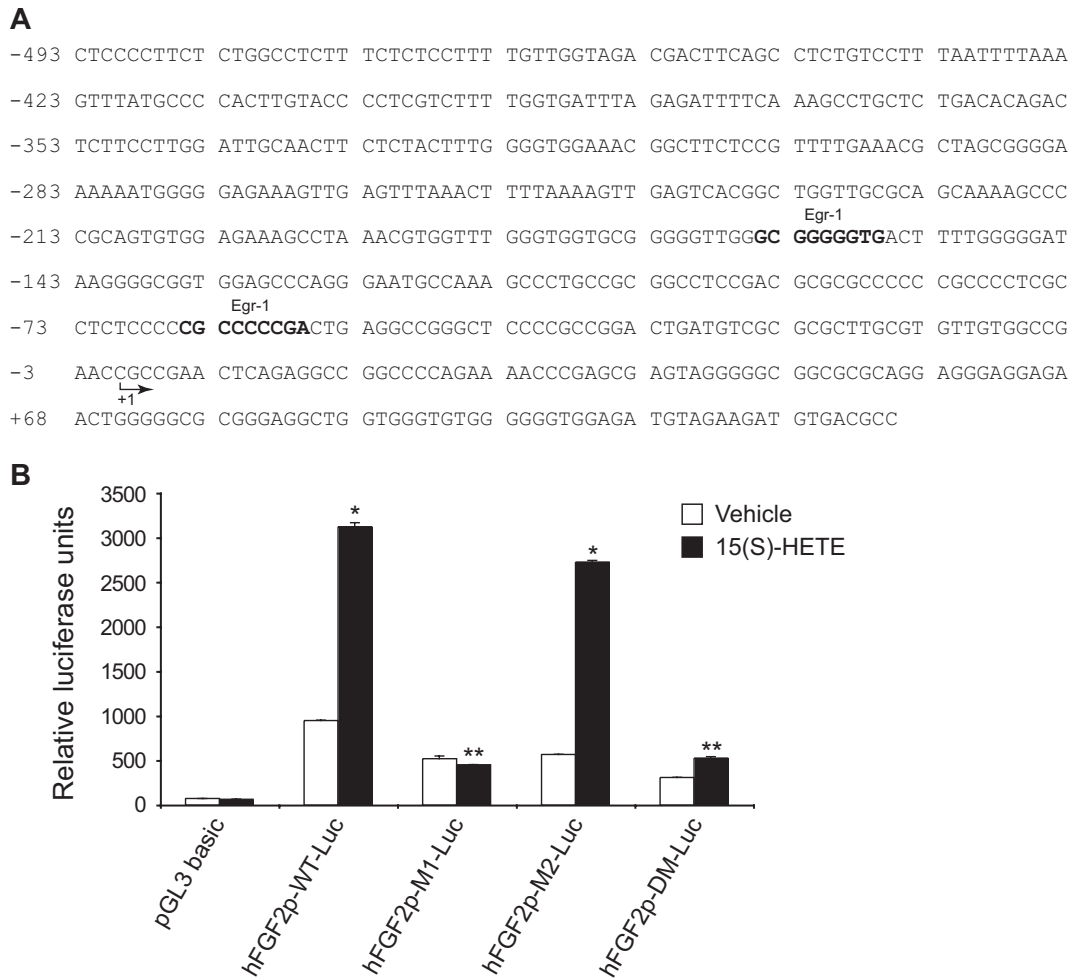
B

Figure 5. 15(S)-HETE–induced FGF-2 promoter-luciferase expression requires Egr-1-binding site. (A) Sequence of a 0.5-kb cloned human FGF-2 promoter region showing the Egr-1 binding sites. Sequence in bold represents Egr-1-binding site; +1 indicates transcription start site. (B) HDMVECs were transfected with either empty vector or FGF-2 promoter-luciferase constructs, quiesced, and treated with and without $0.1\,\mu M$ 15(S)-HETE for 30 minutes, and cell extracts were prepared and analyzed for luciferase activity. The bar graph in panel B represents the quantitative analysis of 3 independent experiments. The values are presented as the means $\pm$ SD. $*P < .01$ vs hFGF2p-WT-Luc vehicle control; $**P < .01$ vs hFGF2p-WT-Luc + 15(S)-HETE. hFGF2p-WT-Luc indicates human FGF-2 promoter-luciferase construct; hFGF2p-M1-Luc, human FGF-2 promoter-luciferase construct with mutation in the first Egr-1 binding site from the transcriptional start site; hFGF2p-M2-Luc, human FGF-2 promoter-luciferase construct with mutation in the second Egr-1 binding site from the transcriptional start site; hFGF2p-DM-Luc, human FGF-2 promoter-luciferase construct with mutations in both the Egr-1 binding sites.

transcriptional factor.[29] 15(S)-HETE induced the expression of Egr-1 mRNA in a time-dependent manner, with a 5-fold increase at 30 minutes and declining thereafter (Figure 1A). The induction of Egr-1 by 15(S)-HETE also was confirmed at protein level as determined by Western blot analysis. A 3- to 4-fold increase in Egr-1 levels was observed at 30 minutes in response to 15(S)-HETE (Figure 1B). Adenovirus-mediated expression of dominant-negative Egr-1 inhibited 15(S)-HETE–induced HDMVEC migration and tube-like structure formation (Figure 1C-D). Consistent with its effects on HDMVEC migration and tube-like structure formation, 15(S)-HETE induced angiogenesis in a Matrigel plug model, and it was attenuated by dn-Egr-1, as determined by double immunofluorescence staining for CD31 and vWF and measuring hemoglobin levels (Figure 1E).

To understand the mechanism(s) by which 15(S)-HETE induces the expression of Egr-1, we tested the role of Src. Consistent with our previous observations,[25] 15(S)-HETE stimulated tyrosine phosphorylation of Src in a time-dependent manner (Figure 2A). Interference with Src activation via adenovirus-mediated expression of its dominant-negative mutant significantly blocked 15(S)-HETE–induced Egr-1 expression both at mRNA and protein levels

(Figure 2B). Adenovirus-mediated expression of dnSrc also blocked 15(S)-HETE–induced HDMVEC migration and tube-like structure formation as well as Matrigel plug angiogenesis (Figure 2C-E).

Jin et al[32] have indicated a direct role for Egr-1 in the regulation of FGF-2. Hence, to find the downstream effector molecules of Egr-1 in mediating 15(S)-HETE–induced angiogenesis, we examined the role of FGF-2. 15(S)-HETE induced FGF-2 mRNA expression rapidly, as determined by quantitative reverse-transcription (QRT)-PCR. Maximum increase in FGF-2 mRNA expression occurred at 30 minutes after treatment with 15(S)-HETE (Figure 3A). The rapid increase in FGF-2 mRNA levels was confirmed at the protein level as well. Western blot analysis and ELISA data showed a 3- to 5-fold increase in the expression and release of FGF-2 by 15(S)-HETE acutely with maximum effect at 30 minutes (Figure 3B-C). In addition, blockade of either Src or Egr-1 via adenovirus-mediated expression of their dominant-negative mutants suppressed 15(S)-HETE–induced FGF-2 expression both at mRNA and protein levels (Figure 4A-C). To understand the molecular mechanisms of FGF-2 regulation by 15(S)-HETE, 0.5 kb of human FGF-2 promoter was cloned and analyzed for transcription factor binding sites by TRANSFAC search.
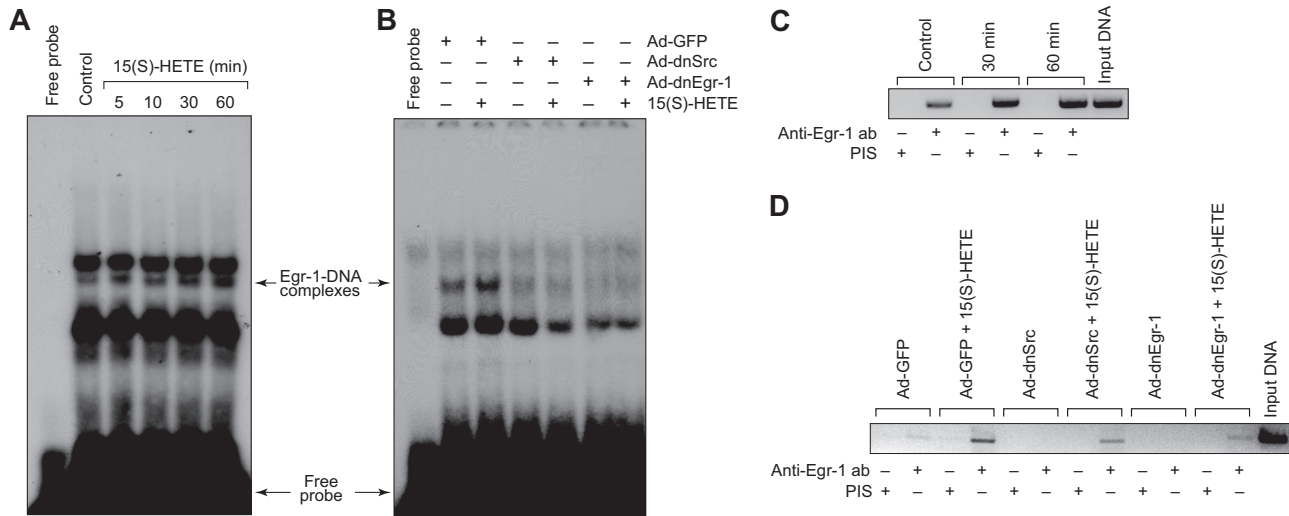
Figure 6. Egr-1 binds to FGF-2 promoter in response to 15(S)-HETE both in vitro and in vivo in Src-dependent manner. (A,C) Quiescent HDMVECs were treated with and without 15(S)-HETE (0.1μM) for the indicated time periods, and either nuclear extracts were prepared and analyzed by EMSA for DNA binding activity in vitro with the use of [^{32}P]-labeled double stranded oligonucleotide probe that corresponds to the Egr-1 binding site proximal to the transcriptional start site in the FGF-2 promoter (A) or processed for ChIP analysis of Egr-1 binding to FGF-2 promoter in vivo (C). (B,D) HDMVECs that were transduced with Ad-GFP, Ad-dnSrc, or Ad-dnEgr-1 with a moi of 40 and quiesced were treated with and without 15(S)-HETE (0.1μM) for 30 minutes and either nuclear extracts were prepared and analyzed by EMSA for DNA binding activity as described in panel A (B) or processed for ChIP analysis of Egr-1 binding to FGF-2 promoter in vivo (D).

TRANSFAC analysis revealed the presence of 2 Egr-1 binding sites in the promoter (Figure 5A).

To further characterize the promoter, the Egr-1 binding sites were mutated and tested for their involvement in 15(S)-HETE–induced FGF-2 promoter-luciferase reporter gene activity. Site-directed mutation of Egr-1 binding site proximal to transcriptional start site abolished 15(S)-HETE–induced FGF-2 promoter-luciferase reporter gene activity (Figure 5B). EMSA analysis with Egr-1 elements proximal to transcriptional start site as a [^{32}P]-labeled probe demonstrated that 15(S)-HETE induced Egr-1 binding to this site in a time-dependent manner with maximum effect at 30 minutes (Figure 6A). In addition, dominant-negative Src or Egr-1 blocked 15(S)-HETE–induced Egr-1 DNA binding activity (Figure 6B). To confirm this result further, we performed the ChIP assay. As shown in Figure 6C, 15(S)-HETE induced Egr-1 binding to FGF-2 promoter in a time-dependent manner with approximately a 2-fold increase at 30 minutes. Adenovirus-mediated expression of either dnSrc or dnEgr-1 completely prevented Egr-1 binding to the FGF-2 promoter in response to 15(S)-HETE (Figure 6D).

To explore the functional role of FGF-2 in 15(S)-HETE–induced angiogenesis, we used its neutralizing antibodies. Neutralizing anti–FGF-2 antibodies blocked 15(S)-HETE–induced HDMVEC migration and tube-like structure formation as well as Matrigel plug angiogenesis (Figure 7A-C). To obtain additional evidence for the role of 15(S)-HETE in the regulation of angiogenesis, we used 12/15-LOX$^{-/-}$ mice. AA, the substrate for cyclooxygenases, lipoxygenases, and epoxygenases, although inducing Matrigel plug angiogenesis in WT mice, failed to influence a similar effect in 12/15-LOX$^{-/-}$ mice (Figure 8A-B). However, the addition of 15(S)-HETE (5μM) to the Matrigel restored the angiogenic stimulus in 12/15-LOX$^{-/-}$ mice (Figure 8A-B). This finding suggests that AA-induced angiogenesis requires its conversion via the 12/15-LOX pathway. To gain additional evidence in support of this notion, we measured the capacity of these plugs to convert AA to 15(S)-HETE. Matrigel plugs were retrieved 7 days after injection from both WT and 12/15-LOX$^{-/-}$ mice that received

either vehicle or AA supplementation at the time of injection, minced, incubated with 10μM AA and 10μM ionomycin for 3 hours, and assayed for 15(S)-HETE by EIA. As shown in Figure 8C, Matrigel plugs from WT mice that received AA supplementation produced several fold greater levels of 15(S)-HETE compared with Matrigel plugs from either control WT or 12-LOX$^{-/-}$ mice or 12-LOX$^{-/-}$ mice that received AA supplementation.

Discussion

The important findings of the present study are as follows. 15(S)-HETE induced Egr-1 expression in HDMVECs. Dominant-negative mutant-mediated blockade of Egr-1 attenuated the effects of 15(S)-HETE on HDMVEC migration and tube-like structure formation as well as Matrigel plug angiogenesis. 15(S)-HETE–induced expression of Egr-1 requires Src activation, and suppression of Src via forced expression of its dominant-negative mutant inhibited the migration and tube-like structure formation of HDMVECs as well as Matrigel plug angiogenesis. 15(S)-HETE induced FGF-2 expression rapidly via Src-mediated production of Egr-1. Cloning and TRANSFAC analysis of human FGF-2 promoter revealed the presence of 2 Egr-1 binding sites, and 15(S)-HETE induced Egr-1 binding to FGF-2 promoter both in vitro and in vivo in a manner that is dependent on Src activation. Site-directed mutagenesis demonstrated that between the 2 Egr-1 binding sites, the one that is proximal to transcriptional start site is crucial in mediating the effects of 15(S)-HETE on FGF-2 promoter-luciferase reporter gene activity. Blockade of FGF-2 via its neutralizing antibodies suppressed the migration and tube-like structure formation of HDMVECs and Matrigel plug angiogenesis. Although AA, the substrate for cyclooxygenases, lipoxygenases, and epoxygenases, induced angiogenesis in WT mice, it failed to stimulate a similar angiogenic response in 12/15-LOX$^{-/-}$ mice, which was rescued by 15(S)-HETE. These findings clearly show that 15(S)-HETE–induced angiogenesis requires Src-mediated Egr-1–dependent rapid induction of expression of FGF-2.
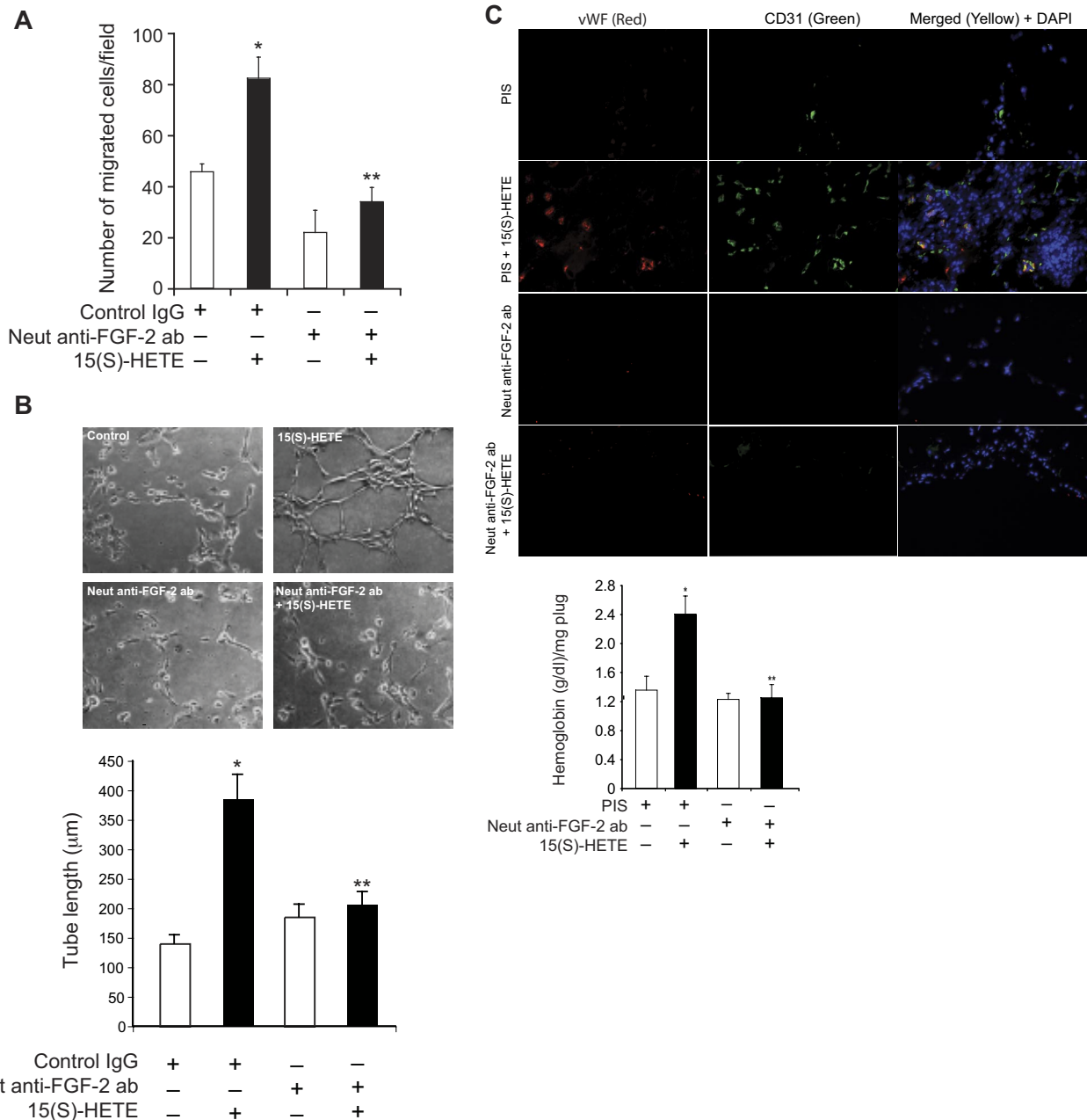
Figure 7. FGF-2 mediates 15(S)-HETE–induced angiogenesis. (A-B) Quiescent HDMVECs were treated with normal serum or neutralizing anti–FGF-2 antibodies (3 μg/mL) for 30 minutes at 37°C followed by washing with medium 131. The cells were then subjected to 15(S)-HETE (0.1μM)–induced migration (A) or tube-like structure formation (B) in the presence and absence of 3 μg/mL of preimmune serum or neutralizing anti–FGF-2 antibodies. (C) C57BL/6 mice were injected subcutaneously with 0.5 mL of Matrigel premixed with vehicle or 5μM 15(S)-HETE in combination with 20 μg/mL preimmune serum or neutralizing anti–FGF-2 antibodies. One week later, the animals were sacrificed, and the Matrigel plugs were harvested from underneath the skin and either processed for vWF and CD31 expression by double immunofluorescence staining using their specific antibodies or analyzed for hemoglobin content using Drabkin reagent. The bar graphs represent the quantitative analysis of 3 independent experiments or 6 plugs from 6 animals. The values are presented as the mean ± SD. *$P < .01$ vs control (normal serum); **$P < .01$ vs 15(S)-HETE (normal serum + 15(S)-HETE).

The role of 15-LOX1 and its murine ortholog, 12/15-LOX, in the pathogenesis of both atherosclerosis and restenosis has been demonstrated.[17-19] Besides its involvement in the oxidation of low-density lipoprotein, the other mechanisms by which 15-LOX1 influences the pathogenesis of these vessel wall diseases are largely unknown. In this aspect, work from our laboratory showed that 15(S)-HETE, a preferential product of 15-LOX1/2, possesses the capacity to influence angiogenesis.[24-26,38] 12(S)-HETE, the AA metabolite of 12/15-LOX, also has been reported to stimulate angiogenesis.[39] In addition, upon incubation with AA atherosclerotic arteries produced 15(S)-HETE preferentially.[16,40] Recently, we have shown that forced expression of 15-LOX2 in rat vascular smooth muscle cells or 15-LOX1 in balloon-injured arteries led to production of only 15(S)-HETE.[41,42] Many reports also revealed that angiogenesis plays a critical role in the progression of atherosclerosis and restenosis.[34,35]

Our findings showed that 12/15-LOX$^{-/-}$ mice fail to exhibit an angiogenic response to AA compared with WT mice. However, the addition of 15(S)-HETE to the Matrigel restored the angiogenic response in these mice. These observations imply
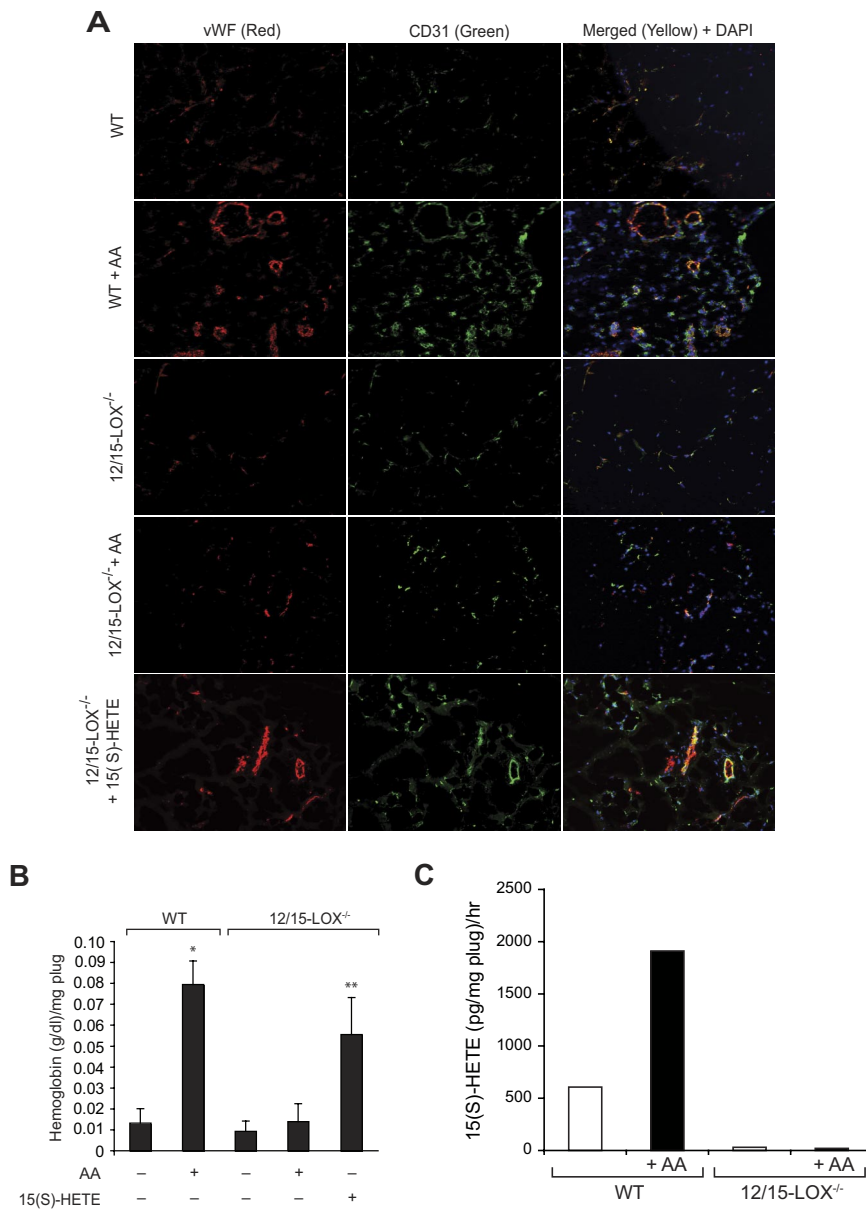
Figure 8. 12/15-LOX$^{-/-}$ mice show lack of angiogenic response to AA. (A-B) Wild-type and 12/15-LOX$^{-/-}$ mice were injected subcutaneously with 0.5 mL of Matrigel premixed with vehicle, 5μM AA, or 5μM 15(S)-HETE as indicated. One week later, the animals were sacrificed, and the Matrigel plugs were harvested from underneath the skin and either processed for vWF and CD31 by double immunofluorescence staining by the use of their specific antibodies (A) or analyzed for hemoglobin content with Drabkin reagent (B). (C) Wild-type and 12/15-LOX$^{-/-}$ mice were injected subcutaneously with 0.5 mL of Matrigel premixed with vehicle or 5μM AA. One week later, the Matrigel plugs were retrieved from animals, minced, incubated with 10μM AA and 10μM ionomycin, and 15(S)-HETE production was measured by EIA. The bar graphs represent the quantitative analysis of 6 plugs from 6 animals. The values are presented as the mean ± SD. *$P < .01$ vs WT control. **$P < .01$ vs WT control or 12/15-LOX$^{-/-}$ control or 12/15-LOX$^{-/-}$ + AA.

that conversion of AA to 15(S)-HETE is essential for induction of angiogenesis. In fact, these conclusions were further reinforced by the findings that Matrigel plugs from only WT mice that were supplemented with AA but not either control WT mice or 12/15-LOX$^{-/-}$ mice with or without AA supplementation possess the capacity to produce 15(S)-HETE. These results also infer that the angiogenic endothelial cells convert AA to 15(S)-HETE. Previous studies by others[17,18] have shown that 12/15-LOX$^{-/-}$ mice develop diminished atherosclerosis in response to a high-fat diet and reduced restenosis in response to vascular injury compared with WT mice. Hence, on the basis of these observations, one can assume that 15(S)-HETE by its capacity to induce angiogenesis may be an important mediator in the pathogenesis of these vascular lesions.

The authors of several studies[29,43] have shown that FGF-2 plays a major role in angiogenesis. In addition, a role for Egr-1 in the regulation of FGF-2 expression has been reported in many cell types, including endothelial cells and cardiac myocytes.[29,32] The present findings also show a role for Egr-1 in 15(S)-HETE–induced

FGF-2 expression, and Src appears to be involved in this transcriptional up-regulation of FGF-2 upstream to Egr-1. In addition, the EMSA and ChIP analysis indicated that Egr-1 binds to FGF-2 promoter directly both in vitro and in vivo. Cloning and characterization of human FGF-2 promoter revealed the presence of 2 Egr-1 binding sites and the Egr-1 binding site that is proximal to transcriptional start site is essential for 15(S)-HETE–induced FGF-2 promoter-luciferase reporter gene activity.

The authors of other studies[32,44] have shown that depending on agonist used, either both the Egr-1 binding sites at −57 nt and −157 nt or the latter site is involved in FGF-2 promoter activity.[32,44] Thus, our results provide a mechanism for 15(S)-HETE–induced expression of FGF-2 in HDMVECs. A large body of evidence[45,46] indicates that FGF-2 is produced in atherosclerotic and restenotic arteries and that neutralizing antibodies inhibit injury-induced vascular wall remodeling. Because we and others[16,40-42] previously demonstrated that atherosclerotic and restenotic arteries produce 15(S)-HETE

abundantly, it is possible that 15(S)-HETE may be a contributing factor in the expression of FGF-2 in these vascular diseases. In fact, it was shown that inhibition of 15-LOX1 via a pharmacologic approach attenuates atherosclerosis.[47,48] In view of these observations, one can assume that 15-LOX1/2, via their role in the production of 15(S)-HETE, may be a crucial mediator in the progression of peripheral vascular diseases such as atherosclerosis and restenosis. In conclusion, in this report we provide mechanistic evidence for the ability of 15-LOX1/2 products of AA in the stimulation of angiogenesis.

Acknowledgments

Authorship

Contribution: V.K.-S. performed ChIP assays, EIA, EMSA, tube formation assay, and assisted in data analysis and the writing of the paper; J.N. performed QRT-PCR, Western blotting, ELISA, and the migration assay; D.W. performed immunohistochemistry and the Matrigel plug angiogenesis assay; D.V.Q. performed cloning; Q.Z. performed QRT-PCR; N.K.S. performed Matrigel plug angiogenesis; J.S. performed Western blot analysis; S.K. amplified and purified adenovirus; and G.N.R. designed the experiments, interpreted the results, and wrote the paper.

Conflict-of-interest disclosure: The authors declare no competing financial interests.

Correspondence: Gadiparthi N. Rao, PhD, Department of Physiology, University of Tennessee Health Science Center, 894 Union Ave, Memphis, TN 38163; e-mail: grao@physio1.utmem.edu.

References

1. Sigal E, Craik CS, Highland E, et al. Molecular cloning and primary structure of human 15-lipoxygenase. *Biochem Biophys Res Commun.* 1988; 157(2):457-464.

2. Brash AR, Boeglin WE, Chang MS. Discovery of a second 15S-lipoxygenase in humans. *Proc Natl Acad Sci U S A.* 1997;94(12):6148-6152.

3. Bryant RW, Bailey JM, Schewe T, Rapoport SM. Positional specificity of a reticulocyte lipoxygenase. Conversion of arachidonic acid to 15-S-hydroperoxy-eicosatetraenoic acid. *J Biol Chem.* 1982;257(11):6050-6055.

4. Chang MS, Schneider C, Roberts RL, et al. Detection and subcellular localization of two 15S-lipoxygenases in human cornea. *Invest Ophthalmol Vis Sci.* 2005;46(3):849-856.

5. Kelavkar UP, Nixon JB, Cohen C, Dillehay D, Eling TE, Badr KF. Overexpression of 15-lipoxygenase-1 in PC-3 human prostate cancer cells increases tumorigenesis. *Carcinogenesis.* 2001; 22(11):1765-1773.

6. Shappell SB, Olson SJ, Hannah SE, et al. Elevated expression of 12/15-lipoxygenase and cyclooxygenase-2 in a transgenic mouse model of prostate carcinoma. *Cancer Res.* 2003;63(9): 2256-2267.

7. Tang S, Bhatia B, Maldonado CJ, et al. Evidence that arachidonate 15-lipoxygenase 2 is a negative cell cycle regulator in normal prostate epithelial cells. *J Biol Chem.* 2002;277(18):16189-16201.

8. Bhatia B, Maldonado CJ, Tang S, et al. Subcellular localization and tumor-suppressive functions of 15-lipoxygenase 2 (15-LOX2) and its splice variants. *J Biol Chem.* 2003;278(27):25091-25100.

9. Liu B, Maher RJ, De Jonckheere JP, et al. 12(S)-HETE increases the motility of prostate tumor cells through selective activation of PKC alpha. *Adv Exp Med Biol.* 1997;400B:707-718.

10. Tang DG, Renaud C, Stojakovic S, Diglio CA, Porter A, Honn KV. 12(S)-HETE is a mitogenic factor for microvascular endothelial cells: its potential role in angiogenesis. *Biochem Biophys Res Commun.* 1995;211(2):462-468.

11. Shappell SB, Gupta RA, Manning S, et al. 15S-Hydroxyeicosatetraenoic acid activates peroxisome proliferator-activated receptor gamma and inhibits proliferation in PC3 prostate carcinoma cells. *Cancer Res.* 2001;61(2):497-503.

12. Shureiqi I, Chen D, Lotan R, et al. 15-Lipoxygenase-1 mediates nonsteroidal anti-inflammatory drug-induced apoptosis independently of cyclooxygenase-2 in colon cancer cells. *Cancer Res.* 2000; 60(24):6846-6850.

13. Shureiqi I, Jiang W, Zuo X, et al. The 15-lipoxygenase-1 product 13-S-hydroxyoctadecadienoic acid down-regulates PPAR-delta to induce apoptosis in colorectal cancer cells. *Proc Natl Acad Sci U S A.* 2003;100(17):9968-9973.

14. Heydeck D, Upston JM, Viita H, Yla-Herttuala S, Stocker R. Oxidation of LDL by rabbit and human 15-lipoxygenase: prevalence of nonenzymatic reactions. *J Lipid Res.* 2001;42(7):1082-1088.

15. Zhao L, Funk CD. Lipoxygenase pathways in atherogenesis. *Trends Cardiovasc Med.* 2004; 14(5):191-195.

16. Henriksson P, Hamberg M, Diczfalusy U. Formation of 15-HETE as a major hydroxyeicosatetraenoic acid in the atherosclerotic vessel wall. *Biochim Biophys Acta.* 1985;834(2):272-274.

17. Cyrus T, Witztum JL, Rader DJ, et al. Disruption of the 12/15-lipoxygenase gene diminishes atherosclerosis in apo E-deficient mice. *J Clin Invest.* 1999;103(11):1597-1604.

18. Gu JL, Pei H, Thomas L, et al. Ribozyme-mediated inhibition of rat leukocyte-type 12-lipoxygenase prevents intimal hyperplasia in balloon-injured rat carotid arteries. *Circulation.* 2001;103(10):1446-1452.

19. Harats D, Shaish A, George J, et al. Overexpression of 15-lipoxygenase in vascular endothelium accelerates early atherosclerosis in LDL receptor-deficient mice. *Arterioscler Thromb Vasc Biol.* 2000;20(9):2100-2105.

20. Augustin AJ, Grus FH, Koch F, Spitznas M. Detection of eicosanoids in epiretinal membranes of patients suffering from proliferative vitreoretinal diseases. *Br J Ophthalmol.* 1997;81(1):58-60.

21. Zhu D, Medhora M, Campbell WB, Spitzbarth N, Baker JE, Jacobs ER. Chronic hypoxia activates lung 15-lipoxygenase, which catalyzes production of 15-HETE and enhances constriction in neonatal rabbit pulmonary arteries. *Circ Res.* 2003; 92(9):992-1000.

22. Setty BN, Ganley C, Stuart MJ. Effect of changes in oxygen tension on vascular and platelet hydroxyacid metabolites. II. Hypoxia increases 15-hydroxyeicosatetraenoic acid, a proangiogenic metabolite. *Pediatrics.* 1985;75(5):911-915.

23. Graeber JE, Glaser BM, Setty BN, Jerdan JA, Walenga RW, Stuart MJ. 15-Hydroxyeicosatetraenoic acid stimulates migration of human retinal microvessel endothelium in vitro and neovascularization in vivo. *Prostaglandins.* 1990;39(6):665-673.

24. Bajpai AK, Blaskova E, Pakala SB, et al. 15(S)-HETE production in human retinal microvascular endothelial cells by hypoxia: novel role for MEK1

in 15(S)-HETE–induced angiogenesis. *Invest Ophthalmol Vis Sci.* 2007;48(11):4930-4938.

25. Zhang B, Cao H, Rao GN. 15(S)-hydroxyeicosatetraenoic acid induces angiogenesis via activation of PI3K-Akt-mTOR-S6K1 signaling. *Cancer Res.* 2005;65(16):7283-7291.

26. Srivastava K, Kundumani-Sridharan V, Zhang B, Bajpai AK, Rao GN. 15(S)-hydroxyeicosatetraenoic acid-induced angiogenesis requires STAT3-dependent expression of VEGF. *Cancer Res.* 2007;67(9):4328-4336.

27. Abdel-Malak NA, Mofarrahi M, Mayaki D, Khachigian LM, Hussain SN. Early growth response-1 regulates angiopoietin-1–induced endothelial cell proliferation, migration, and differentiation. *Arterioscler Thromb Vasc Biol.* 2009; 29(2):209-216.

28. Grotegut S, von Schweinitz D, Christofori G, Lehembre F. Hepatocyte growth factor induces cell scattering through MAPK/Egr-1-mediated upregulation of Snail. *EMBO J.* 2006;25(15): 3534-3545.

29. Fahmy RG, Dass CR, Sun LQ, Chesterman CN, Khachigian LM. Transcription factor Egr-1 supports FGF-dependent angiogenesis during neovascularization and tumor growth. *Nat Med.* 2003;9(8):1026-1032.

30. Du B, Fu C, Kent KC, et al. Elevated Egr-1 in human atherosclerotic cells transcriptionally represses the transforming growth factor-beta type II receptor. *J Biol Chem.* 2000;275(50):39039-39047.

31. Lowe HC, Fahmy RG, Kavurma MM, Baker A, Chesterman CN, Khachigian LM. Catalytic oligodeoxynucleotides define a key regulatory role for early growth response factor-1 in the porcine model of coronary in-stent restenosis. *Circ Res.* 2001;89(8):670-677.

32. Jin Y, Sheikh F, Detillieux KA, Cattini PA. Role for early growth response-1 protein in alpha(1)-adrenergic stimulation of fibroblast growth factor-2 promoter activity in cardiac myocytes. *Mol Pharmacol.* 2000;57(5):984-990.

33. Zhao HY, Ooyama A, Yamamoto M, et al. Molecular basis for the induction of an angiogenesis inhibitor, thrombospondin-1, by 5-fluorouracil. *Cancer Res.* 2008;68(17):7035-7041.

34. Shah F, Balan P, Weinberg M, et al. Contrast-enhanced ultrasound imaging of atherosclerotic carotid plaque neovascularization: a new surrogate marker of atherosclerosis? *Vasc Med.* 2007; 12(4):291-297.

35. Khurana R, Zhuang Z, Bhardwaj S, et al. Angiogenesis-dependent and independent phases of

intimal hyperplasia. *Circulation.* 2004;110(16): 2436-2443.

36. Madden SL, Cook DM, Morris JF, Gashler A, Sukhatme VP, Rauscher FJ 3rd. Transcriptional repression mediated by the WT1 Wilms tumor gene product. *Science.* 1991;253(5027):1550-1553.

37. Cheranov SY, Karpurapu M, Wang D, Zhang B, Venema RC, Rao GN. An essential role for SRC-activated STAT-3 in 14,15-EET-induced VEGF expression and angiogenesis. *Blood.* 2008; 111(12):5581-5591.

38. Cheranov SY, Wang D, Kundumani-Sridharan V, et al. The 15(S)-hydroxyeicosatetraenoic acid-induced angiogenesis requires Janus kinase 2-signal transducer and activator of transcription-5B-dependent expression of interleukin-8. *Blood.* 2009;113(23):6023-6033.

39. Tang DG, Renaud C, Stojakovic S, Diglio CA, Porter A, Honn KV. 12(S)-HETE is a mitogenic factor for microvascular endothelial cells: its potential role in angiogenesis. *Biochem Biophys Res Commun.* 1995;211(2):462-468.

40. Simon TC, Makheja AN, Bailey JM. Formation of 15-hydroxyeicosatetraenoic acid (15-HETE) as the predominant eicosanoid in aortas from Watanabe heritable hyperlipidemic and cholesterol-fed rabbits. *Atherosclerosis.* 1989;75(1):31-38.

41. Chava KR, Karpurapu M, Wang D, et al. CREB-mediated IL-6 expression is required for 15(S)-hydroxyeicosatetraenoic acid-induced vascular smooth muscle cell migration. *Arterioscler Thromb Vasc Biol.* 2009;29(6):809-815.

42. Potula HSK, Wang D, Quyen DV, et al. Src-dependent STAT-3-mediated expression of monocyte chemoattractant protein-1 is required for 15(S)-hydroxyeicosatetraenoic acid-induced vascular smooth muscle cell migration. *J Biol Chem.* 2009;284(45):31142-31155.

43. Poole TJ, Finkelstein EB, Cox CM. The role of FGF and VEGF in angioblast induction and migration during vascular development. *Dev Dyn.* 2001;220(1):1-17.

44. Wang D, Mayo MW, Baldwin AS Jr. Basic fibroblast growth factor transcriptional autoregulation requires EGR-1. *Oncogene.* 1997;14(19):2291-2299.

45. Hughes SE, Crossman D, Hall PA. Expression of basic and acidic fibroblast growth factors and their receptor in normal and atherosclerotic human arteries. *Cardiovasc Res.* 1993;27(7):1214-1219.

46. Lindner V, Lappi DA, Baird A, Majack RA, Reidy MA. Role of basic fibroblast growth factor in vascular lesion formation. *Circ Res.* 1991;68(1):106-113.

47. Cornicelli JA, Trivedi BK. 15-Lipoxygenase and its inhibition: a novel therapeutic target for vascular disease. *Curr Pharm Des.* 1999;5(1):11-20.

48. Bocan TM, Rosebury WS, Mueller SB, et al. A specific 15-lipoxygenase inhibitor limits the progression and monocyte-macrophage enrichment of hypercholesterolemia-induced atherosclerosis in the rabbit. *Atherosclerosis.* 1998;136(2):203-216.